Phenotype of SARS-CoV-2-specific T-cells in COVID-19 patients with acute respiratory distress syndrome

Daniela Weiskopf[1#], Katharina S. Schmitz[2#], Matthijs P. Raadsen[2], Alba Grifoni[1], Nisreen M.A. Okba[2], Henrik Endeman[3], Johannes P.C. van den Akker[3], Richard Molenkamp[2], Marion P.G. Koopmans[2], Eric C.M. van Gorp[2], Bart L. Haagmans[2], Rik L. de Swart[2], Alessandro Sette[1,4,5$] & Rory D. de Vries[2$]*

[1] Center for Infectious Disease, La Jolla Institute for Immunology, La Jolla, CA92037, USA

[2] Department of Viroscience, Erasmus MC, Rotterdam, the Netherlands

[3] Department of Intensive Care, Erasmus MC, Rotterdam, the Netherlands

[4] Department of Pathology, University of California, San Diego, CA92037, USA

[5] Department of Medicine, University of California, San Diego, CA92037, USA

[#] equal first author contribution

[$] equal last author contribution

* author for correspondence: r.d.devries@erasmusmc.nl

Running title: SARS-CoV-2-specific T-cells in ARDS patients

Summary

COVID-19 is associated with lymphopenia and ‘cytokine storm’, but there is a scarcity of information on specific cellular immune responses to SARS-CoV-2. Here, we characterized SARS-CoV-2-specific $CD4^+$ and $CD8^+$ T-cells in patients hospitalized with acute respiratory distress syndrome (ARDS).

Abstract

SARS-CoV-2 has been identified as the causative agent of a global outbreak of respiratory tract disease (COVID-19). In some patients the infection results in moderate to severe acute respiratory distress syndrome (ARDS), requiring invasive mechanical ventilation. High serum levels of IL-6 and an immune hyperresponsiveness referred to as a ‘cytokine storm’ have been associated with poor clinical outcome. Despite the large numbers of cases and deaths, information on the phenotype of SARS-CoV-2-specific T-cells is scarce. Here, we detected SARS-CoV-2-specific $CD4^+$ and $CD8^+$ T cells in 100% and 80% of COVID-19 patients, respectively. We also detected low levels of SARS-CoV-2-reactive T-cells in 20% of the healthy controls, not previously exposed to SARS-CoV-2 and indicative of cross-reactivity due to infection with ‘common cold’ coronaviruses. Strongest T-cell responses were directed to the surface glycoprotein (spike, S), and SARS-CoV-2-specific T-cells predominantly produced effector and Th1 cytokines, although Th2 and Th17 cytokines were also detected. Collectively, these data stimulate further studies into the role of T-cells in COVID-19, support vaccine design and facilitate the evaluation of vaccine candidate immunogenicity.

45 **Introduction**

46 A novel coronavirus, named SARS-CoV-2, has been identified as the causative
47 agent of a global outbreak of respiratory tract disease, referred to as COVID-19
48 (Chan et al., 2020; Huang et al., 2020). On May 1st, over 3 million cases and more
49 than 230,000 deaths were reported globally. COVID-19 is characterized by fever,
50 cough, dyspnea and myalgia (Huang et al., 2020), but in some patients the infection
51 results in moderate to severe acute respiratory distress syndrome (ARDS), requiring
52 invasive mechanical ventilation for a period of several weeks. COVID-19 patients
53 may present with lymphopenia (Chen et al., 2020; Huang et al., 2020), but the
54 disease has also been associated with immune hyperresponsiveness referred to as
55 a 'cytokine storm' (Mehta et al., 2020). A transient increase in co-expression of CD38
56 and HLA-DR by T-cells, a phenotype of $CD8^+$ T-cell activation in response to viral
57 infection, was observed concomitantly (Xu et al., 2020). This increase in both $CD4^+$
58 and $CD8^+$ $CD38^+$HLA-DR^+ T-cells preceded resolution of clinical symptoms in a non-
59 severe, recovered, COVID-19 patient (Thevarajan et al., 2020).

60

61 Despite the large numbers of cases and deaths, there is a scarcity of information on
62 the phenotype of SARS-CoV-2-specific T-cells. Spike surface glycoprotein (S-), M-
63 and NP-specific T-cells were detected in PBMC from convalescent COVID-19
64 patients (Ni et al., 2020). Virus-specific T-cells have also been detected after
65 exposure to the related SARS-CoV and MERS-CoV, although few studies have
66 characterized cellular responses in human patients. For SARS-CoV-specific $CD4^+$ T-
67 cells it was reported that the S glycoprotein accounted for nearly two thirds of T-cell
68 reactivity, N and M also accounted for limited reactivity (Li et al., 2008). For MERS-

69 CoV-specific $CD4^+$ T-cells responses targeting S, N and a pool of M and E peptides
70 have been reported (Zhao et al., 2017).
71
72 Here, we stimulated peripheral blood mononuclear cells (PBMC) from ten COVID-19
73 patients with ARDS, collected up to three weeks after admission to the intensive care
74 unit (ICU), with MegaPools (MP) of overlapping or prediction-based peptides
75 covering the SARS-CoV-2 proteome (Grifoni et al., 2020). We detected SARS-CoV-
76 2-specific $CD4^+$ and $CD8^+$ T-cells in 10/10 and 8/10 COVID-19 patients, respectively.
77 Peptide stimulation of healthy control (HC) PBMC samples collected before the
78 outbreak in most cases resulted in undetectable responses, although some potential
79 cross-reactivity due to infection with 'common cold' coronaviruses was observed.
80 SARS-CoV-2-specific T-cells predominantly produced effector and Th1 cytokines,
81 although Th2 and Th17 cytokines were also detected.
82
83 **Results & Discussion**
84 We included ten COVID-19 patients with moderate to severe ARDS in this study. All
85 patients were included in the study shortly after ICU admission; self-reported illness
86 varied between 5 and 14 days before inclusion (Figure 1a). Patients were between
87 49 and 72 years old (average 58.9 ± 7.2 years) and of mixed gender (4 female, 6
88 male). All patients tested SARS-CoV-2 positive by RT-PCR and were ventilated
89 during their stay at the ICU. At the time of writing, 5 patients were transferred out of
90 the ICU (case 1, 2, 4, 6 and 7), 3 patients were still in follow-up (case 5, 9 and 10), 1
91 patient was discharged (case 8) and 1 patient was deceased (case 3). Case 4 was
92 deceased 4 days after transfer out of the ICU. Patients were treated with lung
93 protective ventilation using the higher PEEP/lower FiO_2 table of the ARDSnet and

94 restrictive volume resuscitation. They received antibiotics as a part of a treatment
95 regimen aimed at selective decontamination of the digestive tract. Furthermore, all
96 patients received chloroquine, lopinavir, ritonavir and / or corticosteroids for a brief
97 period of time around admission to the ICU (Figure 1a).
98
99 Phenotyping analysis of PBMC collected 14 days post inclusion via flow cytometry
100 indicated that COVID-19 patients presented with low percentages of $CD3^+$ T-cells in
101 peripheral blood, corresponding to the previously reported lymphopenia (12.1 ± 8.7%
102 in COVID-19 vs 44.3 ± 7.1% in HC, $p<0.0001$, Figure 1b) (Chen et al., 2020; Huang
103 et al., 2020). CD4:CD8 ratios were increased in COVID-19 patients when compared
104 to HC (5.5 ± 3.0 in COVID-19 vs 2.3 ± 0.9 in HC, $p=0.0106$, Figure 1c).
105
106 PBMC from COVID-19 ARDS patients were stimulated with three different peptide
107 MPs: MP_S, MP_CD4_R and two MP_CD8 pools. MP_S contained 221 overlapping
108 peptides (15-mers overlapping by 10 amino acids) covering the entire S glycoprotein
109 and can stimulate both $CD4^+$ and $CD8^+$ T-cells. MP_CD4_R contained 246 HLA
110 class II predicted epitopes covering all viral proteins except S, specifically designed
111 to activate $CD4^+$ T-cells. The two MP_CD8 pools combined contained 628 HLA class
112 I predicted epitopes covering all SARS-CoV-2 proteins, specifically designed to
113 activate $CD8^+$ T-cells (Grifoni et al., 2020). Results obtained with MP_CD8_A and
114 MP_CD8_B have been concatenated and shown as a single stimulation in Figure 2,
115 results obtained with separate stimuli are shown in Supplementary Figure 2. In
116 addition to stimulation of PBMC from COVID-19 ARDS patients, ten HC were
117 included in this study as negative controls. PBMC from healthy controls were
118 obtained before 2020 and could therefore not contain SARS-CoV-2-specific T-cells,

however they potentially contain cross-reactive T-cells induced by circulating seasonal ‘common cold’ coronaviruses (Kissler et al., 2020).

Stimulation of PBMC collected 14 days post inclusion with the different peptide pools led to consistent detection of $CD4^+$ and / or $CD8^+$ SARS-CoV-2-specific T-cells in COVID-19 ARDS patients (Figure 2, Supplementary Figure 2 and Table 1). Specific activation of $CD4^+$ and $CD8^+$ T-cells was measured via cell surface expression of CD69 and CD137; phenotyping of memory subsets was based on surface expression of CD45RA and CCR7 (Supplementary Figure 1).

Stimulation of PBMC with MP_S and MP_CD4_R led to consistent activation of SARS-CoV-2-specific $CD4^+$ T-cells (Figure 2a and b) in PBMC obtained from COVID-19 ARDS patients. Significant responses were detected when activation percentages after stimulation with MP_S and MP_CD4_R were compared with the vehicle control (DMSO). To allow comparison between HC and COVID-19 ARDS patients, we corrected the MP-specific activation percentages by subtracting the value obtained in the DMSO stimulation. Significant T-cell responses were observed in COVID-19 ARDS patients when compared with HC (0.64% in COVID-19 vs 0.02% in HC, $p<0.0001$ for MP_S and 0.29% in COVID-19 vs 0.02% in HC, $p=0.0002$ for MP_CD4_R, Figure 2a). The stimulation index (SI) was calculated by dividing the MP-specific responses by the DMSO responses (Supplementary Figure 2a), and donors with a SI > 3 were regarded responders (Table 1). According to this definition all COVID-19 ARDS patients responded to the MP_S and MP_CD4_R pools, whereas only 1/10 and 2/10 of the HC responded, respectively. Overall, the MP_S peptide pool induced stronger responses than the MP_CD4_R peptide pool,

144 indicating that the S glycoprotein is a strong inducer of $CD4^+$ T-cell responses.
145 Phenotyping of $CD4^+CD69^+CD137^+$ activated T-cells identified the majority of these
146 SARS-CoV-2-specific T-cells as central memory T-cells, based on CD45RA and
147 CCR7 expression (T^{CM}). T^{CM} express homing receptors required for extravasation
148 and migration to secondary lymphoid tissues, but also have high proliferative
149 capacity with low dependence on co-stimulation (Mahnke et al., 2013; Sallusto et al.,
150 1999).
151
152 SARS-CoV-2-specific $CD8^+$ T-cells were activated by both the MP_S and MP_CD8
153 peptide pools when compared to vehicle control (Figure 2c and d). Furthermore,
154 significant responses were detected when activation percentages after stimulation
155 with MP_S and MP_CD8 were compared between HC controls and COVID-19
156 ARDS patients after DMSO correction (0.90% in COVID-19 vs 0.03% in HC,
157 p=0.0003 for MP_S and 0.57% in COVID-19 vs 0.03% in HC, p<0.0001 for
158 MP_CD8, Figure 2b). In addition to inducing specific $CD4^+$ T-cells, the S glycoprotein
159 also induced $CD8^+$ T-cell responses. Calculation of the SI identified 8/10 and 4/9 of
160 the COVID-19 ARDS patients as responders to MP_S and MP_CD8, respectively,
161 whereas 1/10 of the HC responded to the MP_S stimulation (Supplementary Figure
162 2, Table 1). Phenotyping of $CD8^+CD69^+CD137^+$ activated T-cells showed that these
163 had a mixed phenotype. The majority of virus-specific $CD8^+$ T-cells was identified as
164 $CCR7^-$ effector memory (T^{EM}) or terminally differentiated effector (T^{EMRA}) (Mahnke et
165 al., 2013). Both these $CD8^+$ effector subsets are potent producers of IFNγ, contain
166 preformed perforin granules for immediate antigen-specific cytotoxicity and home
167 efficiently to peripheral lymphoid tissues (Sallusto et al., 1999).
168

169 As production of pro-inflammatory cytokines can be predictive of clinical outcome for
170 other viral diseases (Wang et al., 2014), we measured antigen-specific production of
171 13 cytokines in cell culture supernatants from PBMC after stimulation. PBMC were
172 stimulated with the respective peptide pools, cytokine production after MP_S
173 stimulation is shown in Figure 3 and Supplementary Figure 3 as representative data
174 (data for other stimulations not shown). When compared to the vehicle control
175 stimulation, PBMC obtained from COVID-19 ARDS patients specifically produced
176 IFNγ, TNFα, IL-2, IL-5, IL-13, IL-10, IL-9, IL-17a, IL-17f and IL-22 after MP_S
177 stimulation (Figure 3, Supplementary Figure 3).
178
179 When comparing COVID-19 ARDS patients with HC, stimulation of PBMC by the
180 overlapping S peptide pool led to a strong significant production of the Th1 or
181 effector cytokines IFNγ, TNFα and IL-2 in COVID-19 ARDS patients. More
182 characteristic Th2 cytokines (IL-5, IL-13, IL-9 and IL-10) were also consistently
183 detected, albeit at low levels. IL-4 and IL-21 could not be detected at all. IL-6 levels
184 were not different between COVID-19 patients and HC, however results were difficult
185 to interpret because mock stimulation already resulted in high IL-6 expression.
186 Antigen-specific production of cytokines related to a Th17 response was mixed;
187 PBMC from COVID-19 ARDS patients produced significantly more IL-17a and IL-22
188 than HC; this was not observed for IL-17f.
189
190 In general, stimulation of PBMC from COVID-19 ARDS patients with MP led to a
191 dominant production Th1 or effector cytokines (IFNγ, TNFα, IL-2), but Th2 (IL-5, IL-
192 13, IL-9, IL-10) and Th17 cytokines could also be detected (IL-17a, IL-17f and IL-22).
193 Although not enough COVID-19 ARDS patients were included in this study to

194 correlate specific T-cell responses to clinical outcome, we did observe differences in
195 cytokine production profiles on a case-per-case basis (Supplementary Figure 3d).
196 Plotting the respective cytokine quantities as a percentage of total cytokine
197 production showed that either IL-6 (case 3, 5 and 9), TNFα (case 1, 3 and 9), IL-2
198 (case 8) or IFNγ (case 2, 4, 6, 7 and 10) dominated the response.
199
200 Finally, we studied the kinetics of development of virus-specific humoral and cellular
201 immune response in eight COVID-19 ARDS patients included in this study (case 1 –
202 8). Real time RT-PCR detection of SARS-CoV-2 genomes in respiratory tract
203 samples showed a decreasing trend over time (Figure 4a, ANOVA repeated
204 measures $p<0.001$), whereas virus-specific serum IgG antibody levels, measured by
205 RBD ELISA, showed a significant increase (Figure 4b, ANOVA repeated measures,
206 $p<0.001$). Concomitantly, SARS-CoV-2-specific T-cells were detected in all patients
207 at multiple time-points and frequencies of virus-specific responder cells increased
208 significantly over time (Figure 4c, ANOVA repeated measures, $p<0.001$).
209
210 Collectively, these data provide information on the phenotype, breadth and kinetics
211 of virus-specific cellular immune responses in COVID-19 ARDS patients. We provide
212 evidence that SARS-CoV-2-specific $CD4^+$ and $CD8^+$ T-cells appear in blood of
213 ARDS patients in the first two weeks post onset of symptoms, and their frequency
214 increases over time. SARS-CoV-2-specific $CD4^+$ T-cells in blood typically had a
215 central memory phenotype, whereas $CD8^+$ T-cells had a more effector phenotype.
216 Consistent production in response to viral antigen of IFNγ, TNFα, IL-2, IL-5, IL-13, IL-
217 9, IL-10, IL-17a, IL-17f and IL-22 was observed, with a dominant production of the
218 effector and Th1 cytokines. Due to limitations in the number of PBMC that could be

219 obtained from severe COVID-19 ARDS patients in an ICU setting, we could not
220 resolve which cells were responsible for production of which cytokine by intracellular
221 cytokine staining.
222
223 Elevated levels of IL-6 in patient plasma have been correlated to respiratory failure in
224 COVID-19 patients (Herold et al., 2020). Although we could not detect increased
225 specific production of IL-6 in PBMC stimulated with peptide pools due high
226 background production in controls (potentially due to *in vivo* activation), we detected
227 a dominant IL-6 and TNFα response in cell culture supernatants from the patient
228 deceased due to respiratory failure (case 3). To determine the role of T-cells in
229 COVID-19, it is crucial that the cell types responsible for the production of IL-6 and
230 the concomitant 'cytokine storm' are identified in large comparative cohort studies.
231
232 We included PBMC obtained from ten buffycoats obtained before the SARS-CoV-2
233 pandemic as negative HC. In some instances, reactive T-cells were detected in HC
234 after MP stimulation, both on basis of T-cell activation and cytokine production. Since
235 PBMC from these HC could not contain SARS-CoV-2-specific T-cells, we
236 hypothesize that these responses were cross-reactive and had been induced by
237 circulating seasonal 'common cold' coronaviruses. If we consider samples with a SI
238 > 3 as responders, we identified 2 out of 10 HC (20%) to have these cross-reactive
239 T-cells. This is in good accordance with a recent report on the presence of virus-
240 specific $CD4^+$ T-cells in COVID-19 patients, which reported the presence of SARS-
241 CoV-2-reactive T-cells in 34% of the HC (Braun et al., 2020). The role of pre-existing
242 SARS-CoV-2-reactive T-cells as a correlate of protection or pathology is unclear,
243 and needs to be addressed in prospective studies.

Novel SARS-CoV-2 vaccines are currently in development and mainly focus on the surface glycoprotein S as an antigen for efficient induction of virus-specific neutralizing antibodies. We now show that S can also be a potent immunogen for inducing virus-specific $CD4^+$ and $CD8^+$ T-cells. Whether presence and certain phenotypes of T-cells are correlated to a 'good' or 'bad' prognosis remains to be determined. Collectively, these novel data are important for vaccine design and will facilitate the evaluation of future vaccine immunogenicity.

Author contributions

DW, AG, RLdS, AS and RDdV conceived and planned the experiments. DW, KSS, MPR, NMAO, RM and ECMvG contributed to sample preparation. DW, KSS, MPR, AG, NMAO, HE, JPCvsA, RM and RDdV carried out the experiments. DW, KSS, AG, MPGK, BLH, RLdS, AS and RDdV contributed to the interpretation of the results. RDdV took the lead in writing the manuscript, DW, KSS and RLdS contributed significantly. All authors provided critical feedback and helped shape the research, analysis and manuscript.

Acknowledgements

We thank all health care workers and laboratory personnel who contributed to treatment and diagnosis of these and other COVID-19 patients. Specifically, we thank Jeroen van Kampen, Corine Geurts van Kessel, Annemiek van der Eijk and Marshall Lammers for their contributions to these studies. This work has received funding from the European Union's Horizon 2020 research and innovation programme under grant agreements No. 874735 (VEO) (MPGK, EvG and MPR).

Competing interest statement

The authors declare no competing interests.

273 **Tables**

274

		Activation (SI)			
		CD4+ T-cells		CD8+ T-cells	
	Paper ID	MP_S	MP_CD4_R	MP_S	MP_CD8
HC	HC_1	2.0	1.7	1.0	1.0
	HC_2	0.8	0.9	0.9	1.0
	HC_3	0.9	0.9	1.6	1.0
	HC_4	1.7	1.9	1.1	1.1
	HC_5	1.4	1.3	3.0	2.6
	HC_6	8.3	3.6	3.1	1.8
	HC_7	1.4	1.4	0.9	1.1
	HC_8	1.1	2.6	1.2	1.1
	HC_9	2.4	3.8	1.8	1.3
	HC_10	1.7	1.4	1.0	0.9
	total	**1/10**	**2/10**	**1/10**	**0/10**
COVID-19	Case 1	22.0	17.0	4.5	3.8
	Case 2	5.4	4.4	8.4	ND
	Case 3	33.4	18.9	6.7	1.5
	Case 4	29.8	12.6	4.5	3.4
	Case 5	123.3	43.0	1.0	1.1
	Case 6	28.2	5.4	48.0	2.5
	Case 7	57.4	58.8	3.2	5.8
	Case 8	28.6	23.0	1.7	1.2
	Case 9	25.2	3.5	3.7	1.5
	Case 10	18.9	14.4	25.8	15.8
	total	**10/10**	**10/10**	**8/10**	**4/9**

275

276 **Table 1. Antigen-specific responses shown as stimulation index (SI) for HC and COVID-19**
277 **patients.** Antigen-specific activation of $CD4^+$ and $CD8^+$ T-cells in COVID-19 patients after stimulation
278 for 20 hours with peptide MegaPools (MP) shown as stimulation index (SI). SI is derived by dividing
279 the percentage obtained with specific stimulation (MP) by the percentage obtained with the vehicle
280 control (DMSO), values for respective stimulations are shown in Figure 2. Donors with a SI > 3 are
281 regarded responders to MP stimulation, total responders per stimulation are shown at the bottom of
282 the table. Non-responders (SI < 3) are shown in white background, responders are shown in shades
283 of blue (darker blue equals a higher SI). HC = healthy control.

284

Figures

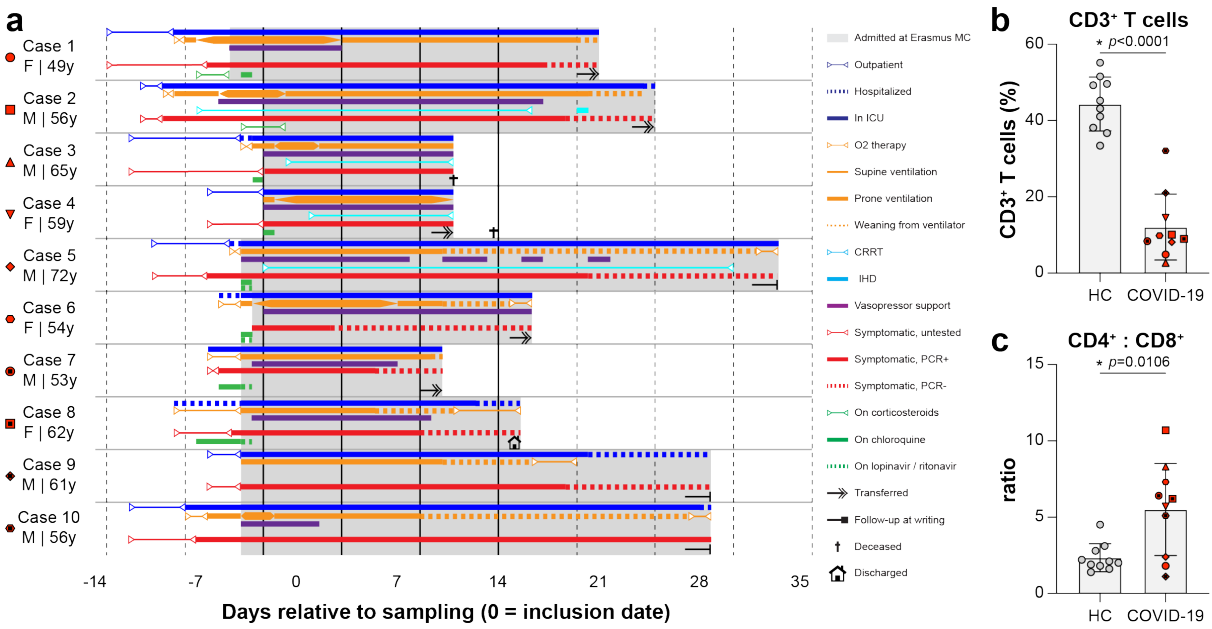

Figure 1. Clinical overview of moderate to severe COVID-19 ARDS patients. (a) Symptoms, hospitalization status, treatment and follow-up of n=10 COVID-19 ARDS patients included in this study. PBMC samples were obtained weekly after admission to the study. Symbols shown next to the cases match throughout all figures. (b) Flow cytometry performed on PBMC collected 14 days post inclusion showed that percentages $CD3^+$ T-cells within the total LIVE gate were significantly lower in COVID-19 patients compared to healthy controls (HC), while (c) CD4:CD8 ratios were significantly higher. Panels b and c show individual values for n=10 patients versus n=10 HC, as well as the mean ± SD. Asterisk denotes a significant difference. HC = healthy control.

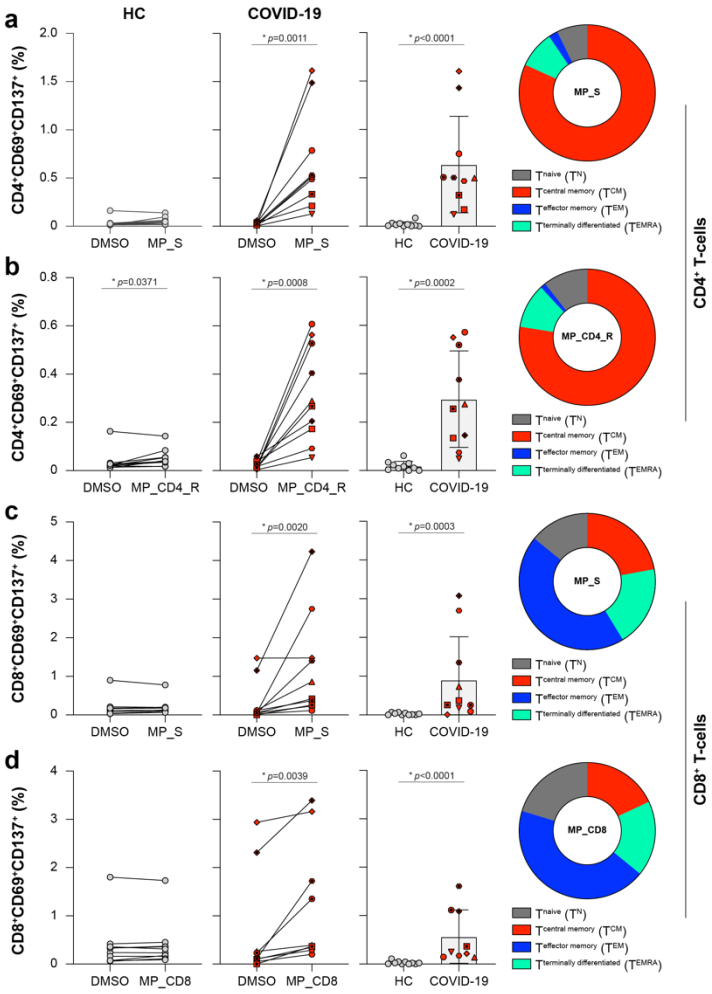

297

298 **Figure 2. SARS-CoV-2-specific T-cell responses in COVID-19 ARDS patients.** (a, b) Antigen-
299 specific activation of $CD4^+$ T-cells after stimulation for 20 hours with MP_S (a) and MP_CD4_R (b),
300 measured via cell surface expression of CD69 and CD137 (gating in supplementary Figure 1). Two
301 left panels show activation percentages (within $CD3^+CD4^+$ or $CD3^+CD8^+$ gate) obtained with the
302 vehicle control (DMSO) and specific stimulation (MP) for HC and COVID-19 patients. The third panel
303 shows the specific activation percentages corrected by subtracting the background present in the
304 DMSO stimulation to allow comparison of both groups. The fourth panel shows the memory
305 phenotype of the $CD69^+CD137^+$ responder cells in a donut diagram. (c, d) Similar layout to panels a
306 and b. Antigen-specific activation of $CD8^+$ T-cells after stimulation for 20 hours with MP_S (c) and
307 MP_CD8 (d). Percentages from MP_CD8 stimulation are based on concatenated analysis of
308 MP_CD8_A and MP_CD8_B, results obtained with separate stimulations are shown in supplementary
309 Figure 2. Panels show individual values for n=10 patients versus n=10 HC, as well as the mean ± SD.
310 Asterisk denotes a significant difference. HC = healthy control. Symbol shapes of COVID-19 patients
311 are identical between panels, and refer back to figure 1.

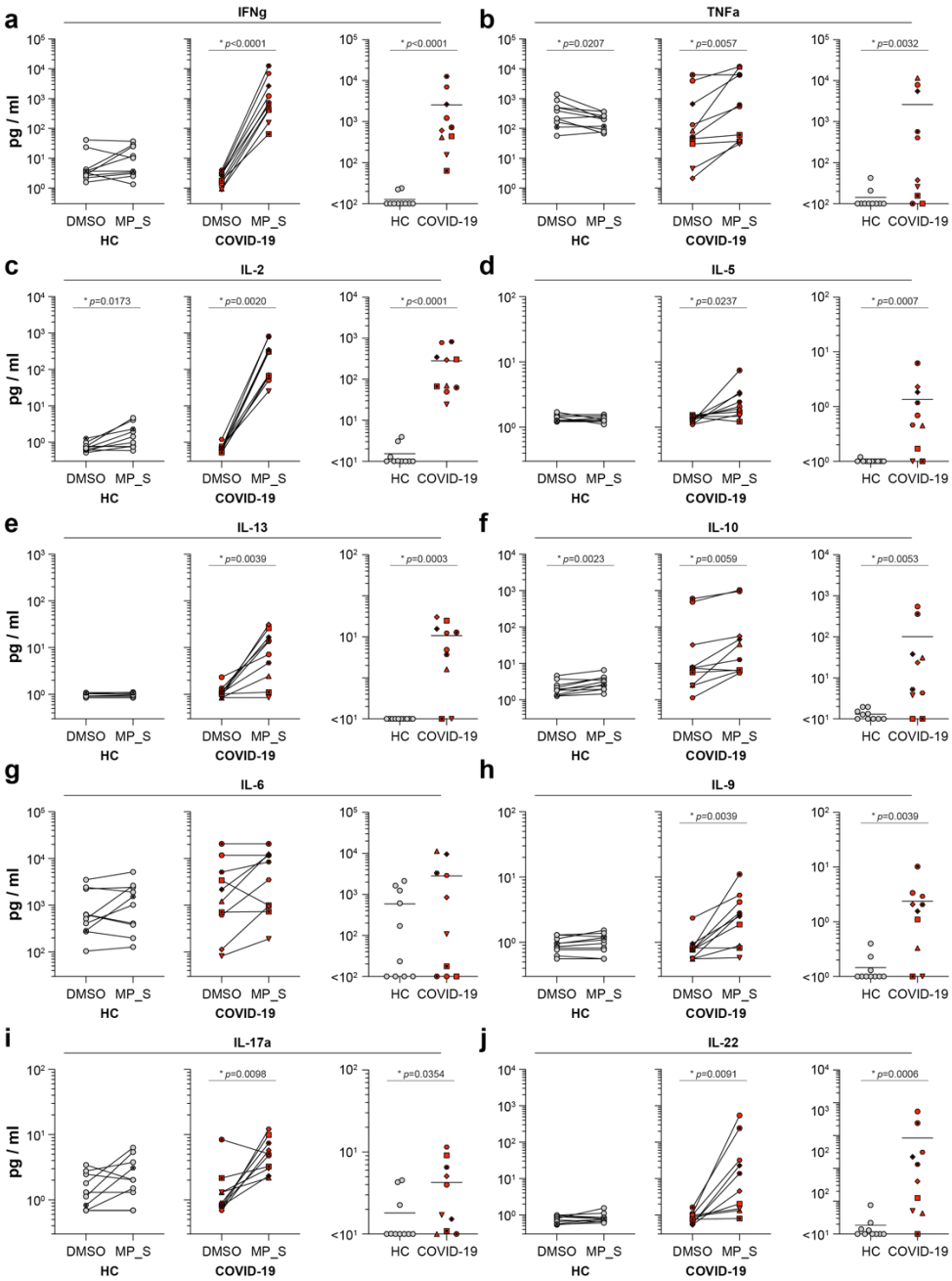

Figure 3. SARS-CoV-2-specific cytokine production in COVID-19 ARDS patients. (a-j) Antigen-specific production of cytokines measured in cell culture supernatants from PBMC stimulated (20 hours) with MP_S. Two left panels show activation percentages obtained with the vehicle control (DMSO) and specific stimulation (MP) for HC and COVID-19 patients. The third panel shows the quantity corrected by subtracting the background present in the DMSO stimulation to allow comparison of both groups. Panels show individual values for n=10 patients versus n=10 HC, as well as the geometric mean. Asterisk denotes a significant difference. HC = healthy control. Additional cytokines (IL-4, IL17f and IL-21) are shown in supplementary Figure 3.

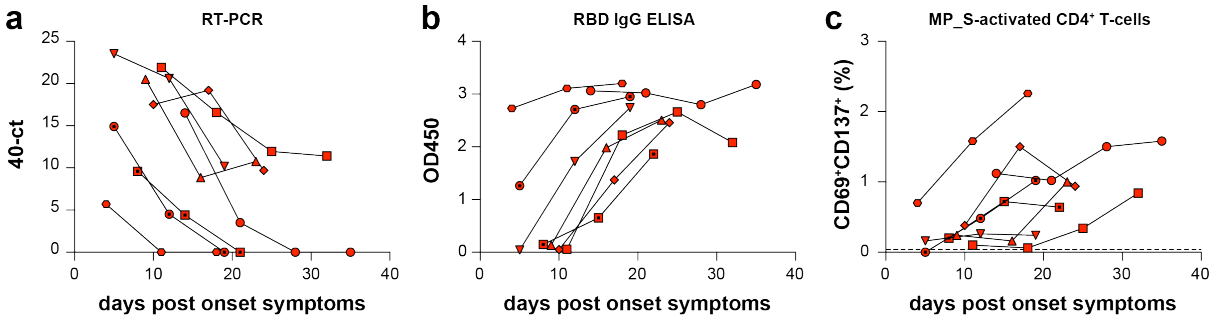

Figure 4. SARS-CoV-2 replication and humoral and cellular immune response kinetics in COVID-19 ARDS patients. (a, b, c) Sequential measurements of SARS-CoV-2 genomes detected in upper respiratory tract samples by real-time RT-PCR (40-ct, a), SARS-CoV-2-specific serum RBD IgG antibody levels detected by ELISA (OD450, b) and percentage SARS-CoV-2-specific $CD4^+$ T-cells after MP_S stimulation of PBMC (c), plotted against days post onset of symptoms. Genome levels showed a significant decrease over time, antibody levels and specific T-cell frequencies significantly increased ($p<0.001$ for all three panels, ANOVA repeated measures). Panels show values for n=8 COVID-19 ARDS patients (case 1 – 8).

Supplementary Figures

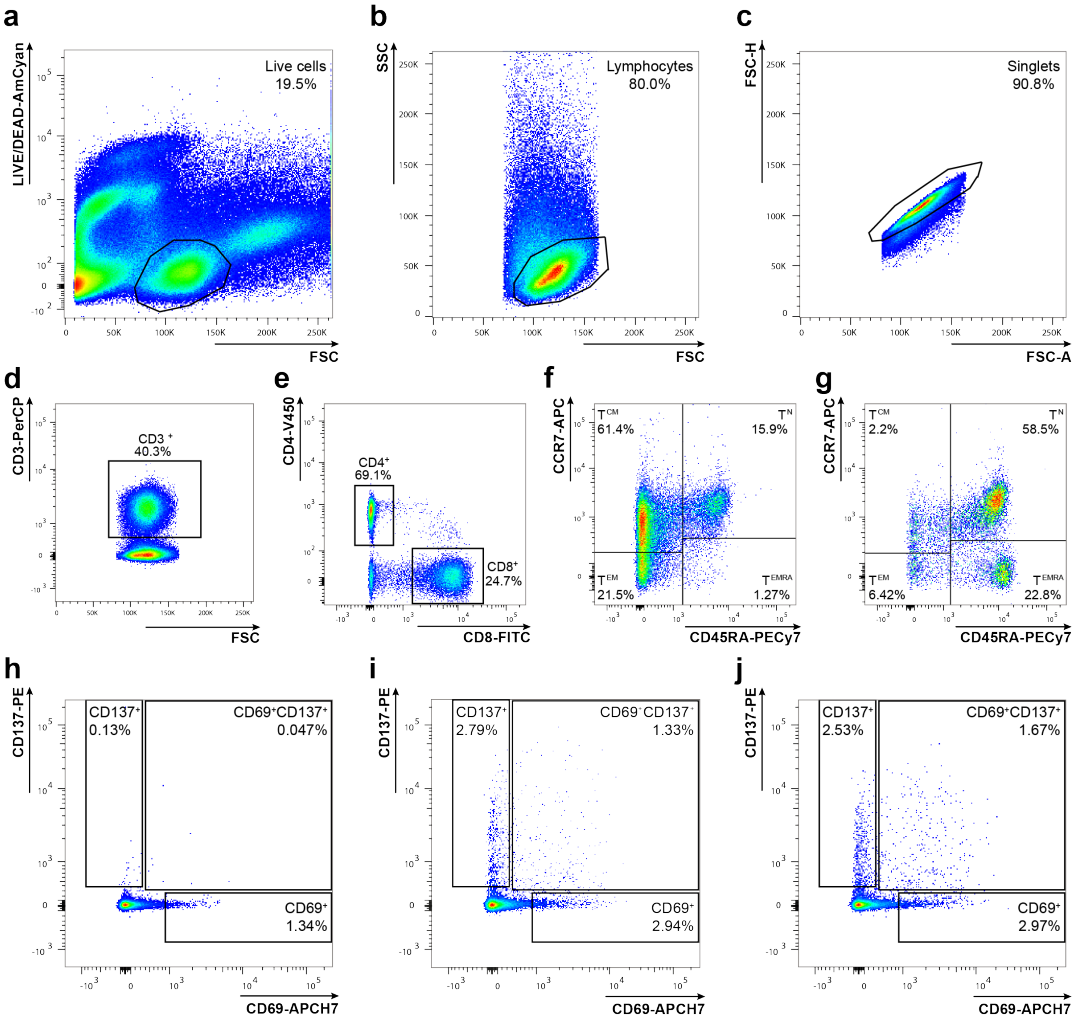

Supplementary Figure 1. Flow cytometry gating strategy. (a-j) Gating strategy for detection of antigen-specific T-cells after stimulation of PBMC. (a) Live cells were selected, (b) followed by the selection of lymphocytes and (c) singlets. (d) $CD3^+$ T-cells were gated and (e) divided into $CD4^+$ and $CD8^+$ T-cells. Both subsets were phenotyped as naïve (T^N), central memory (T^{CM}), effector memory (T^{EM}) or terminally differentiated effectors (T^{EMRA}) on basis of expression of CD45RA and CCR7 (f for $CD4^+$ T-cells, g for $CD8^+$ T-cells). (h-j) Within the different subsets, activated cells were identified via surface upregulation of activation induced markers CD69 and CD137. Percentages of $CD69^+CD137^+$ double positive cells, reflecting activated cells, were used for further analysis. Representative examples of DMSO (vehicle of the MP) (background control, h), CMV peptides (positive control, i) and a MP_S stimulation of PBMC from a COVID-19 patient.

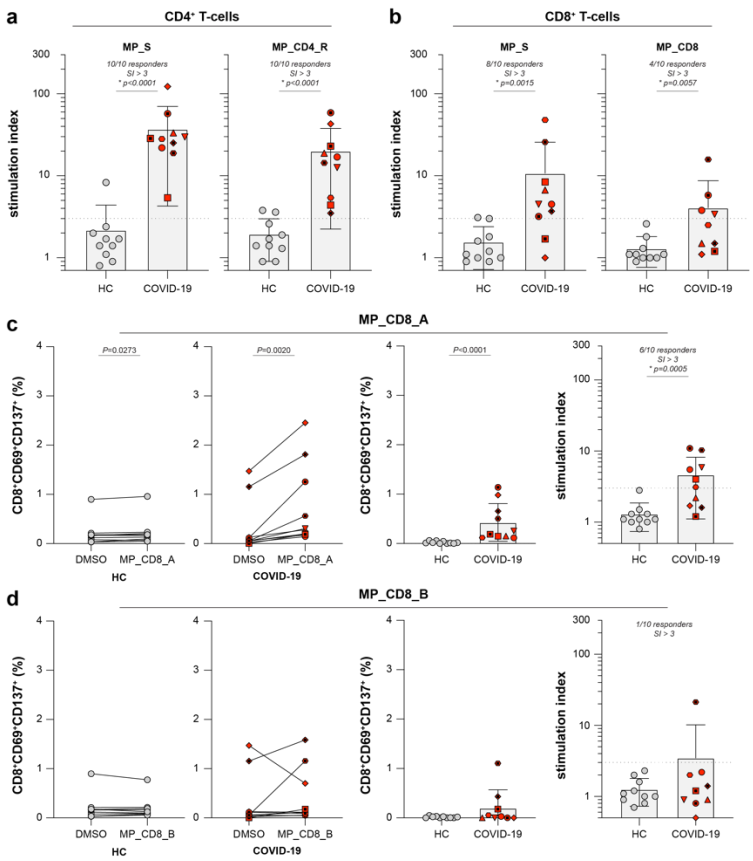

Supplementary Figure 2. SARS-CoV-2-specific T-cell responses in COVID-19 ARDS patients. (a, b) Antigen-specific activation of CD4$^+$ and CD8$^+$ T-cells in COVID-19 patients after stimulation for 20 hours with peptide MegaPools (MP) shown as stimulation index (SI). Stimulation index is derived by dividing the percentage obtained with specific stimulation (MP) by the percentage obtained with the vehicle control (DMSO), values for respective stimulations are shown in Figure 2. Donors with a SI > 3 (dotted line) are regarded responders to MP stimulation. (c, d) Antigen-specific activation of CD8$^+$ T-cells after stimulation for 20 hours with MP_CD8_A (c) and MP_CD8_B (d). The two left panels show activation percentages obtained with the vehicle control (DMSO) and specific stimulation (MP) for HC and COVID-19 patients. The third panel shows the specific activation percentages corrected by subtracting the background present in the DMSO stimulation to allow comparison of both groups. The fourth panel shows the stimulation index derived by dividing the percentage obtained with specific stimulation (MP) by the percentage obtained with the vehicle control (DMSO). Donors with a SI > 3 (dotted line) are regarded responders to MP stimulation. Panels show individual values for n=10 patients versus n=10 HC, as well as the mean ± SD. Asterisk denotes a significant difference. HC = healthy control.

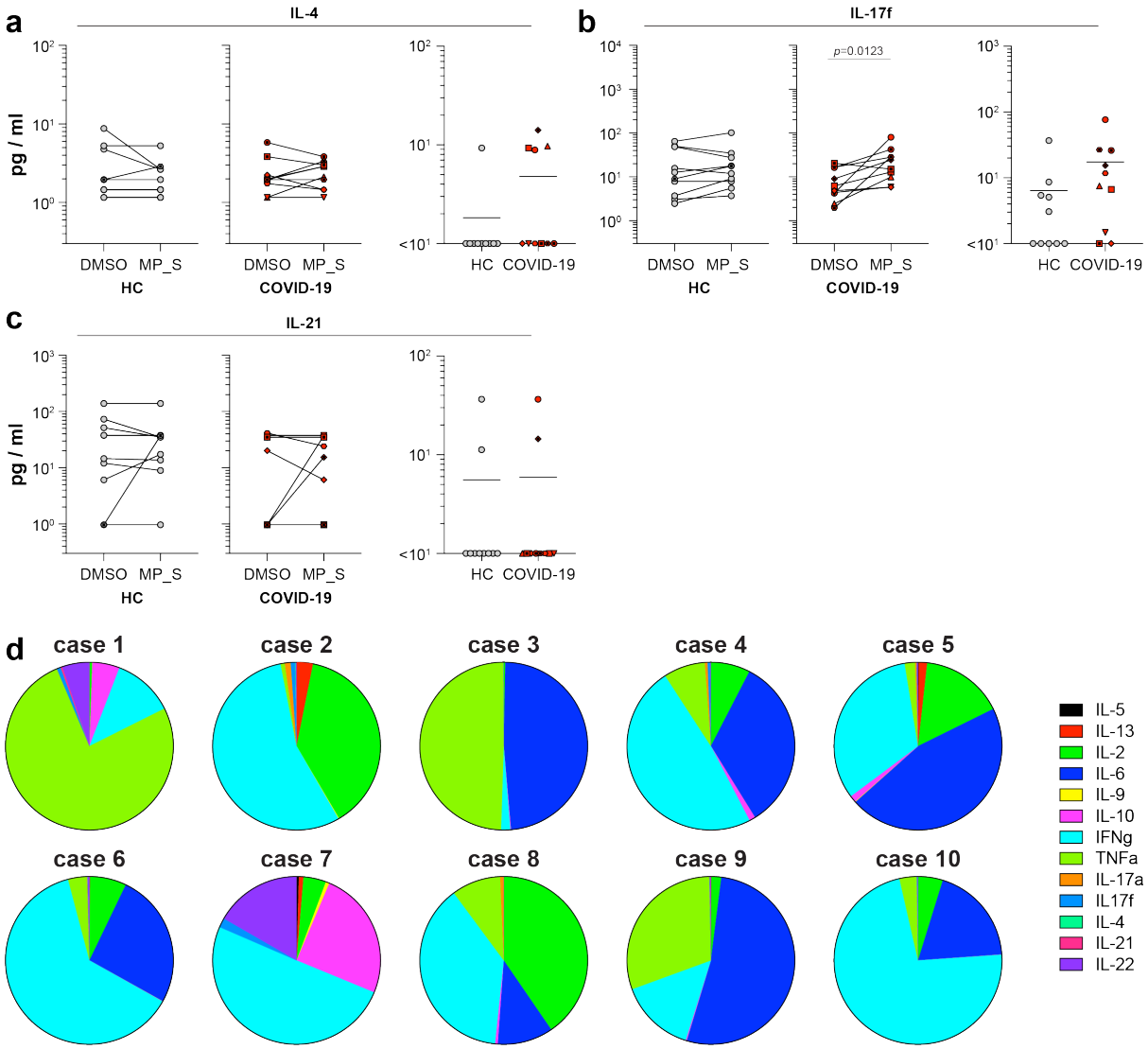

Supplementary Figure 3. SARS-CoV-2-specific cytokine production in COVID-19 ARDS patients. (a-c) Antigen-specific production of cytokines measured in cell culture supernatants from PBMC stimulated (20 hours) with MP_S. Two left panels show activation percentages obtained with the vehicle control (DMSO) and specific stimulation (MP) for HC and COVID-19 patients. Third panel shows the quantity corrected by subtracting the background present in the DMSO stimulation to allow comparison of both groups. Panels show individual values for n=10 patients versus n=10 HC, as well as the geometric mean. Asterisk denotes a significant difference. HC = healthy control. (d) Antigen-specific production of cytokines per COVID-19 case. Circle diagrams represent the total amount of cytokines produced by the respective donor (corrected for DMSO background), quantities of different cytokines are shown as a percentage of whole. Clinical data for cases is described in Figure 1.

375 **Methods**

376

377 **Ethical statement.** Patients admitted into the intensive care unit (ICU) with Acute
378 Respiratory Distress Syndrome (ARDS) resulting from SARS-CoV-2 infection at
379 Erasmus MC, Rotterdam, the Netherlands were included in a biorepository study
380 aimed at ARDS and sepsis in the ICU. The first EDTA blood samples for PBMC
381 isolation were obtained no more than 2 days after admission into the Erasmus MC
382 ICU until 21 days post inclusion for as long as the patient was in the ICU. Patient
383 care and research were conducted in compliance within guidelines of the Erasmus
384 MC and the Declaration of Helsinki. Due to the clinical state of most ARDS patients
385 (*i.e.* intubated, comatose), deferred proxy consent was obtained instead of direct
386 written informed consent from the patients themselves. Retrospective written
387 informed consent was obtained from patients after recovery. The study protocol was
388 approved by the medical ethical committee of Erasmus MC, Rotterdam, the
389 Netherlands (MEC-2017-417 and MEC-2020-0222). For experiments involving
390 healthy control human buffy coats, written informed consent for research use was
391 obtained by the Sanquin Blood Bank (Rotterdam, the Netherlands).

392

393 **Diagnosis.** Real-time RT-PCR on the E-gene was performed as described
394 previously (Corman et al., 2020) on RNA isolated from sputa, nasopharyngeal or
395 oropharyngeal swabs by MagnaPure (Roche diagnostics, The Netherlands) using
396 the total nucleic acid (TNA) isolation kit.

397

398 **PBMC isolation.** PBMC were isolated from EDTA blood samples. Tubes were
399 centrifuged at 200g for 15 min to separate cellular parts. Plasma-containing fraction

400 was collected, centrifuged at 1200g for 15 minutes, plasma was aliquoted and stored
401 at -20°C. The cellular fraction was reconstituted with phosphate-buffered saline
402 (PBS) and subjected to Ficoll density gradient centrifugation (500g, 30min). PBMC
403 were washed and frozen in 90% fetal bovine serum (FBS) and 10% dimethyl
404 sulfoxide (DMSO, Sigma Life science) at -135°C. Upon use, PBMC were thawed in
405 IMDM (Lonza, Belgium) supplemented with 10% FBS, 100 IU of penicillin/ml, 100 µg
406 of streptomycin/ml (Lonza, Belgium) and 2 mM L-glutamine (Lonza, Belgium) (I10F
407 medium). PBMC were treated with 50 U/ml benzonase (Merck) for 30min at 37°C
408 prior to use in stimulation assays.
409
410 **Epitope MegaPool (MP) design and preparation.** SARS-CoV-2 virus-specific CD4
411 and CD8 peptides were synthesized as crude material (A&A, San Diego, CA),
412 resuspended in DMSO, pooled and sequentially lyophilized as previously
413 reported(Carrasco Pro et al., 2015). SARS-CoV-2 epitopes were predicted using the
414 protein sequences derived from the SARS-CoV-2 reference (GenBank: MN908947)
415 and IEDB analysis-resource as previously described (Dhanda et al., 2019; Grifoni et
416 al., 2020). Specifically, CD4 SARS-CoV-2 epitope prediction was carried out using a
417 previously described approach in Tepitool resource in IEDB (Paul et al., 2015; Paul
418 et al., 2016) similarly to what was previously described (Grifoni et al., 2020), but
419 removing the resulting Spike glycoprotein epitopes from this prediction (CD4-
420 R(remainder) MP, n=246). To investigate in depth Spike-specific $CD4^+$ T-cells,
421 overlapping 15-mer by 10 amino acids have been synthesized and pooled separately
422 (CD-4 S(spike) MP, n=221). CD8 SARS-CoV-2 epitope prediction was performed as
423 previously reported, using the NetMHCpan4.0 algorithm for the top 12 more frequent
424 HLA alleles in the population (HLA-A*01:01, HLA-A*02:01, HLA-A*03:01, HLA-

425 A*11:01, HLA-A*23:01, HLA-A*24:02, HLA-B*07:02, HLA-B*08:01, HLA-B*35:01,
426 HLA-B*40:01, HLA-B*44:02, HLA-B*44:03) and selecting the top 1 percentile
427 predicted epitope per HLA allele (Grifoni et al., 2020). The 628 predicted CD8
428 epitopes were split in two CD8 MPs containing 314 peptides each.
429
430 **SARS-CoV-2 RBD ELISA.** Serum or plasma samples were analyzed for the
431 presence of SARS-CoV-2 specific antibody responses using a validated in-house
432 SARS-CoV-2 receptor binding domain (RBD) IgG ELISA as previously
433 described(Okba et al., 2020). Briefly, ELISA plates were coated with recombinant
434 SARS-CoV-2 RBD protein. Following blocking, samples were added and incubated
435 for 1 hour, after which the plates were washed and a secondary HRP-labelled rabbit
436 anti-human IgG (DAKO) was added. Following a 1 hour incubation, the plates were
437 washed, the signal was developed using TMB, and the OD_{450} was measured for
438 each well. All samples reported here were interrogated for the presence of
439 antibodies on the same plate.
440
441 ***Ex vivo* stimulations.** PBMC were plated in 96-wells U bottom plates at 1 x 10^6
442 PBMC per well in RPMI1640 (Lonza, Belgium) supplemented with 10% human
443 serum, 100 IU of penicillin/ml, 100 µg of streptomycin/ml (Lonza, Belgium) and 2 mM
444 L-glutamine (Lonza, Belgium) (R10H medium) and subsequently stimulated with the
445 described CD4 and CD8 SARS-CoV-2 MPs at 1µg/ml. A stimulation with an
446 equimolar amount of DMSO was performed as negative control, phytohemagglutinin
447 (PHA, Roche, 1µg/ml) and stimulation with a combined CD4 and CD8
448 cytomegalovirus MP (CMV, 1µg/ml) were included as positive controls. Twenty hours
449 after stimulation cells were stained for detection of activation induced markers and

450 subjected to flow cytometry. Supernatants were harvested for multiplex detection of
451 cytokines.
452
453 **Flow cytometry.** Activation-induced markers were quantified via flow cytometry
454 (FACSLyric, BD Biosciences). A surface staining on PBMC was performed with anti-
455 $CD3^{PerCP}$ (BD, clone SK7), anti-$CD4^{V450}$ (BD, clone L200), anti-$CD8^{FITC}$ (DAKO,
456 clone DK25), anti-$CD45RA^{PE\text{-}Cy7}$ (BD, clone L48), anti-$CCR7^{APC}$ (R&D Systems,
457 clone 150503), anti-$CD69^{APC\text{-}H7}$ (BD, clone FN50) and anti-$CD137^{PE}$ (Miltenyi, clone
458 4B4-1). T-cell subsets were identified via the following gating strategy: LIVE $CD3^+$
459 were selected and divided in $CD3^+CD4^+$ and $CD3^+CD8^+$. Within the CD4 and CD8
460 subsets, memory subsets were gated as $CD45RA^+CCR7^+$ (naive, T^n), $CD45RA^-$,
461 $CCR7^+$ (central memory, T^{CM}), $CD45RA^-CCR7^-$ (effector memory, T^{EM}) or
462 $CD45RA^+CCR7^-$ (terminally differentiated effectors, T^{EMRA}). T-cells specifically
463 activated by SARS-CoV-2 were identified by upregulation of CD69 and CD137. An
464 average of 500,000 cells was always acquired, the gating strategy is schematically
465 represented in (Supplementary Figure 1A-J). In analysis, PBMC stimulated with
466 MP_CD8_A and MP_CD8_B were concatenated and analyzed as a single file for
467 SARS-CoV-2-specific responses to MP_CD8.
468
469 **Multiplex detection of cytokines.** Cytokines in cell culture supernatants from *ex*
470 *vivo* stimulations were quantified using a human Th cytokine panel (13-plex) kit
471 (LEGENDplex, Biolegend). Briefly, cell culture supernatants were mixed with beads
472 coated with capture antibodies specific for IL-5, IL-13, IL-2, IL-6, IL-9, IL-10, IFNγ,
473 TNFα, IL-17a, IL-17F, IL-4, IL-21 and IL-22 and incubated for 2 hours. Beads were
474 washed and incubated with biotin-labelled detection antibodies for 1 hour, followed

475 by a final incubation with streptavidin^{PE}. Beads were analyzed by flow cytometry.
476 Analysis was performed using the LEGENDplex analysis software v8.0, which
477 distinguishes between the 13 different analytes on basis of bead size and internal
478 dye. Quantity of each respective cytokine is calculated on basis of intensity of the
479 streptavidin^{PE} signal and a freshly prepared standard curve.
480
481 **Statistical analysis.** For comparison of $CD3^+$ T-cell percentages, CD4:CD8 ratios,
482 $CD69^+CD137^+$ stimulated T-cells and cytokine levels between HC and COVID-19
483 patients all log transformed data was tested for normal distribution. If distributed
484 normally, groups were compared via an unpaired T test. If not distributed normally,
485 groups were compared via a Mann-Whitney test. Comparisons between different
486 stimulations (DMSO versus MP) were performed by paired T-test (normal
487 distribution) or Wilcoxon rank test (no normal distribution). Two-tailed *p* values are
488 reported throughout the manuscript. One way ANOVA repeated measures was used
489 to test for increasing or decreasing trends over sequential time points (0, 7 and 14
490 days post inclusion).
491
492

493 **References**

494

495 Braun, J., L. Loyal, M. Frentsch, D. Wendisch, P. Georg, F. Kurth, S. Hippenstiel, M.
496 Dingeldey, B. Kruse, F. Fauchere, E. Baysal, M. Mangold, L. Henze, R.
497 Lauster, M. Mall, K. Beyer, J. Roehmel, J. Schmitz, S. Miltenyi, M.A. Mueller,
498 M. Witzenrath, N. Suttorp, F. Kern, U. Reimer, H. Wenschuh, C. Drosten,
499 V.M. Corman, C. Giesecke-Thiel, L.-E. Sander, and A. Thiel. 2020. Presence
500 of SARS-CoV-2 reactive T cells in COVID-19 patients and healthy donors.
501 Carrasco Pro, S., J. Sidney, S. Paul, C. Lindestam Arlehamn, D. Weiskopf, B.
502 Peters, and A. Sette. 2015. Automatic Generation of Validated Specific
503 Epitope Sets. *J Immunol Res* 2015:763461.
504 Chan, J.F., S. Yuan, K.H. Kok, K.K. To, H. Chu, J. Yang, F. Xing, J. Liu, C.C. Yip,
505 R.W. Poon, H.W. Tsoi, S.K. Lo, K.H. Chan, V.K. Poon, W.M. Chan, J.D. Ip,
506 J.P. Cai, V.C. Cheng, H. Chen, C.K. Hui, and K.Y. Yuen. 2020. A familial
507 cluster of pneumonia associated with the 2019 novel coronavirus indicating
508 person-to-person transmission: a study of a family cluster. *Lancet* 395:514-
509 523.
510 Chen, G., D. Wu, W. Guo, Y. Cao, D. Huang, H. Wang, T. Wang, X. Zhang, H. Chen,
511 H. Yu, X. Zhang, M. Zhang, S. Wu, J. Song, T. Chen, M. Han, S. Li, X. Luo, J.
512 Zhao, and Q. Ning. 2020. Clinical and immunological features of severe and
513 moderate coronavirus disease 2019. *J Clin Invest* 130:2620-2629.
514 Corman, V.M., O. Landt, M. Kaiser, R. Molenkamp, A. Meijer, D.K. Chu, T. Bleicker,
515 S. Brunink, J. Schneider, M.L. Schmidt, D.G. Mulders, B.L. Haagmans, B. van
516 der Veer, S. van den Brink, L. Wijsman, G. Goderski, J.L. Romette, J. Ellis, M.
517 Zambon, M. Peiris, H. Goossens, C. Reusken, M.P. Koopmans, and C.

518 Drosten. 2020. Detection of 2019 novel coronavirus (2019-nCoV) by real-time
519 RT-PCR. *Euro Surveill* 25:
520 Dhanda, S.K., S. Mahajan, S. Paul, Z. Yan, H. Kim, M.C. Jespersen, V. Jurtz, M.
521 Andreatta, J.A. Greenbaum, P. Marcatili, A. Sette, M. Nielsen, and B. Peters.
522 2019. IEDB-AR: immune epitope database-analysis resource in 2019. *Nucleic*
523 *Acids Res* 47:W502-W506.
524 Grifoni, A., J. Sidney, Y. Zhang, R.H. Scheuermann, B. Peters, and A. Sette. 2020. A
525 Sequence Homology and Bioinformatic Approach Can Predict Candidate
526 Targets for Immune Responses to SARS-CoV-2. *Cell Host Microbe* 27:671-
527 680 e672.
528 Herold, T., V. Jurinovic, C. Arnreich, J.C. Hellmuth, M. von Bergwelt-Baildon, M.
529 Klein, and T. Weinberger. 2020. Level of IL-6 predicts respiratory failure in
530 hospitalized symptomatic COVID-19 patients. *MedRxiv*
531 Huang, C., Y. Wang, X. Li, L. Ren, J. Zhao, Y. Hu, L. Zhang, G. Fan, J. Xu, X. Gu, Z.
532 Cheng, T. Yu, J. Xia, Y. Wei, W. Wu, X. Xie, W. Yin, H. Li, M. Liu, Y. Xiao, H.
533 Gao, L. Guo, J. Xie, G. Wang, R. Jiang, Z. Gao, Q. Jin, J. Wang, and B. Cao.
534 2020. Clinical features of patients infected with 2019 novel coronavirus in
535 Wuhan, China. *Lancet* 395:497-506.
536 Kissler, S.M., C. Tedijanto, E. Goldstein, Y.H. Grad, and M. Lipsitch. 2020.
537 Projecting the transmission dynamics of SARS-CoV-2 through the
538 postpandemic period. *Science*
539 Li, C.K., H. Wu, H. Yan, S. Ma, L. Wang, M. Zhang, X. Tang, N.J. Temperton, R.A.
540 Weiss, J.M. Brenchley, D.C. Douek, J. Mongkolsapaya, B.H. Tran, C.L. Lin,
541 G.R. Screaton, J.L. Hou, A.J. McMichael, and X.N. Xu. 2008. T cell responses
542 to whole SARS coronavirus in humans. *J Immunol* 181:5490-5500.

543 Mahnke, Y.D., T.M. Brodie, F. Sallusto, M. Roederer, and E. Lugli. 2013. The who's
544 who of T-cell differentiation: human memory T-cell subsets. *Eur J Immunol*
545 43:2797-2809.
546 Mehta, P., D.F. McAuley, M. Brown, E. Sanchez, R.S. Tattersall, J.J. Manson, and
547 U.K. Hlh Across Speciality Collaboration. 2020. COVID-19: consider cytokine
548 storm syndromes and immunosuppression. *Lancet* 395:1033-1034.
549 Ni, L., F. Ye, M.-L. Cheng, Y. Feng, Y.-Q. Deng, H. Zhao, P. Wei, J. Ge, M. Gou, X.
550 Li, L. Sun, T. Cao, P. Wang, C. Zhou, R. Zhang, P. Liang, H. Guo, X. Wang,
551 C.-F. Qin, F. Chen, and C. Dong. 2020. Detection of SARS-CoV-2-specific
552 humoral and cellular immunity in COVID-19 convalescent individuals.
553 *Immunity*
554 Okba, N.M.A., M.A. Muller, W. Li, C. Wang, C.H. GeurtsvanKessel, V.M. Corman,
555 M.M. Lamers, R.S. Sikkema, E. de Bruin, F.D. Chandler, Y. Yazdanpanah, Q.
556 Le Hingrat, D. Descamps, N. Houhou-Fidouh, C. Reusken, B.J. Bosch, C.
557 Drosten, M.P.G. Koopmans, and B.L. Haagmans. 2020. Severe Acute
558 Respiratory Syndrome Coronavirus 2-Specific Antibody Responses in
559 Coronavirus Disease 2019 Patients. *Emerg Infect Dis* 26:
560 Paul, S., C.S. Lindestam Arlehamn, T.J. Scriba, M.B. Dillon, C. Oseroff, D. Hinz,
561 D.M. McKinney, S. Carrasco Pro, J. Sidney, B. Peters, and A. Sette. 2015.
562 Development and validation of a broad scheme for prediction of HLA class II
563 restricted T cell epitopes. *J Immunol Methods* 422:28-34.
564 Paul, S., J. Sidney, A. Sette, and B. Peters. 2016. TepiTool: A Pipeline for
565 Computational Prediction of T Cell Epitope Candidates. *Curr Protoc Immunol*
566 114:18 19 11-18 19 24.

567 Sallusto, F., D. Lenig, R. Forster, M. Lipp, and A. Lanzavecchia. 1999. Two subsets
568 of memory T lymphocytes with distinct homing potentials and effector
569 functions. *Nature* 401:708-712.
570 Thevarajan, I., T.H.O. Nguyen, M. Koutsakos, J. Druce, L. Caly, C.E. van de Sandt,
571 X. Jia, S. Nicholson, M. Catton, B. Cowie, S.Y.C. Tong, S.R. Lewin, and K.
572 Kedzierska. 2020. Breadth of concomitant immune responses prior to patient
573 recovery: a case report of non-severe COVID-19. *Nat Med* 26:453-455.
574 Wang, Z., A. Zhang, Y. Wan, X. Liu, C. Qiu, X. Xi, Y. Ren, J. Wang, Y. Dong, M.
575 Bao, L. Li, M. Zhou, S. Yuan, J. Sun, Z. Zhu, L. Chen, Q. Li, Z. Zhang, X.
576 Zhang, S. Lu, P.C. Doherty, K. Kedzierska, and J. Xu. 2014. Early
577 hypercytokinemia is associated with interferon-induced transmembrane
578 protein-3 dysfunction and predictive of fatal H7N9 infection. *Proc Natl Acad*
579 *Sci U S A* 111:769-774.
580 Xu, Z., L. Shi, Y. Wang, J. Zhang, L. Huang, C. Zhang, S. Liu, P. Zhao, H. Liu, L.
581 Zhu, Y. Tai, C. Bai, T. Gao, J. Song, P. Xia, J. Dong, J. Zhao, and F.S. Wang.
582 2020. Pathological findings of COVID-19 associated with acute respiratory
583 distress syndrome. *Lancet Respir Med* 8:420-422.
584 Zhao, J., A.N. Alshukairi, S.A. Baharoon, W.A. Ahmed, A.A. Bokhari, A.M. Nehdi,
585 L.A. Layqah, M.G. Alghamdi, M.M. Al Gethamy, A.M. Dada, I. Khalid, M.
586 Boujelal, S.M. Al Johani, L. Vogel, K. Subbarao, A. Mangalam, C. Wu, P. Ten
587 Eyck, S. Perlman, and J. Zhao. 2017. Recovery from the Middle East
588 respiratory syndrome is associated with antibody and T-cell responses. *Sci*
589 *Immunol* 2: eaan5393.
590